CrossMark

Interannual variability of seasonal rainfall over the Cape south coast of South Africa and synoptic type association

Christien J. Engelbrecht[1,2] · Willem A. Landman[2,3]

Abstract The link between interannual variability of seasonal rainfall over the Cape south coast of South Africa and different synoptic types as well as selected teleconnections is explored. Synoptic circulation over the region is classified into different synoptic types by employing a clustering technique, the self-organizing map (SOM), on daily circulation data for the 33-year period from 1979 to 2011. Daily rainfall data are used to investigate interannual variability of seasonal rainfall within the context of the identified synoptic types. The anomalous frequency of occurrence of the different synoptic types for wet and for dry seasons differs significantly within the SOM space, except for austral spring. The main rainfall-producing synoptic types are to a large extent consistent for wet and dry seasons. The main rainfall-producing synoptic types have a notable larger contribution to seasonal rainfall totals during wet seasons than during dry seasons, consistent with a higher frequency of occurrence of the main rainfall-producing synoptic types during wet seasons compared to dry seasons. Dry seasons are characterized by a smaller contribution to seasonal rainfall totals by all the different synoptic types, but with the largest negative anomalies associated with low frequencies of the main rainfall-producing synoptic types. The frequencies of occurrence of specific configurations of ridging high pressure systems, cut-off lows and tropical-temperate troughs associated with rainfall are positively linked to interannual variability of seasonal rainfall. It is also shown that the distribution of synoptic types within the SOM space is linked to the Southern Annular Mode and El Niño Southern Oscillation, implying some predictability of intraseasonal variability at the seasonal time scale.

Keywords Cape south coast of South Africa · Synoptic types · Interannual rainfall variability · El Niño Southern Oscillation · Southern Annular Mode · Intraseasonal predictability

1 Introduction

Three precipitation regimes are notable over South Africa. Most of the country receives rainfall in austral summer (Barclay et al. 1993; Fauchereau et al. 2009; Crétat et al. 2012; Pohl et al. 2014), with the extreme southwestern area characterized by austral winter rainfall (Reason et al. 2002; Philippon et al. 2012; Pohl et al. 2014). The third precipitation regime is found along the coast in the far south of the country, referred to as the Cape south coast. Here, pronounced seasonality in rainfall is absent and rainfall occurs throughout the year, with small peaks during the transitional seasons (Taljaard 1996; Pohl et al. 2014; Weldon and Reason 2014). Rainfall-producing weather systems characteristic of both the winter and summer rainfall regions of South Africa occur over the Cape south coast, contributing to the region's unique climate. Its unique climate is also linked to local topography and the Agulhas Current and their interaction with regional circulation (Rouault et al. 2002; Singleton and Reason 2006). The interaction between regional circulation, topography and the Agulhas Current is in particularly illustrated during

✉ Christien J. Engelbrecht
 engelbrechtc@arc.agric.za

1 Institute for Soil, Climate and Water, Agricultural Research Council, Pretoria, South Africa

2 Department of Geography, Geoinformatics and Meteorology, University of Pretoria, Pretoria, South Africa

3 Climate Studies, Modelling and Environmental Health, CSIR Natural Resources and Environment, Pretoria, South Africa

events of southerly meridional flow when topographically enhanced uplift of moisture that has been advected over the Agulhas Current occurs. Weather systems responsible for rainfall over this region are cold fronts, west-wind troughs, cut-off lows (COLs), ridging high pressure systems (Taljaard 1996; Favre et al. 2013; Weldon and Reason 2014) and tropical-temperate troughs (Taljaard 1996; Hart et al. 2013). Of these weather systems, ridging high pressure systems, tropical-temperate troughs and COLs are the main rain-producing weather systems of the Cape south coast. The mean contribution of ridging high pressure systems, tropical-temperate troughs and COLs to annual rainfall totals was quantified to be 46, 28 and 16 % respectively by application of a self-organizing map (SOM) (Engelbrecht et al. 2015). It may be noted that COLs occur in combination with ridging high pressure systems and tropical-temperate troughs. COLs are known to be the main cause of extreme rainfall events along the Cape south coast (Taljaard 1985; Singleton and Reason 2006, 2007a, b).

Seasonal-to-interannual variability is an integral characteristic of the climate over southern Africa (Mason and Jury 1997; Reason et al. 2002; Reason and Rouault 2005; Washington and Preston 2006), a region that is also characterized by substantial agricultural practices in the commercial and subsistence sectors. In comparison with rainfall variability studies concerning the summer rainfall region (van Heerden et al. 1988; Jury et al. 1992; Mason and Jury 1997; Cook et al. 2004) where most crops are produced (Malherbe et al. 2014b), and to a lesser extent the winter rainfall region (Reason et al. 2002; Reason and Rouault 2005; Philippon et al. 2012), the Cape south coast has been neglected (Weldon and Reason 2014) with regard to rainfall variability studies. This notion is despite the region being an important agricultural area (e.g. dairy production, livestock farming and forestry). Noteworthy though is the smaller variability in rainfall over the Cape south coast compared to rainfall variability experienced over the winter and summer rainfall regions (Taljaard 1996). However, floods and droughts occur from time to time over the Cape south coast—usually impacting significantly on the region, in particular on agriculture. The flood events that occurred in August 2006 and in November 2007 led to agricultural losses exceeding ZAR 100,000,000 for each of the disasters (Holloway et al. 2012). The same kind of weather system that caused the 2006 and 2007 floods, namely a COL, brought an end to the severe meteorological drought of 2008–2009 that occurred over the region and impacted significantly on both rain-fed and irrigation dependent agriculture (Holloway et al. 2012).

Rainfall variability is the result of changes in the frequency, duration, intensity (Mason and Jury 1997) and location (Hart et al. 2013) of rain-producing weather systems and these attributes can in turn be affected by larger-scale climate modes such as the Southern Annular Mode (SAM) (Reason and Rouault 2005; Malherbe et al. 2014a) and El Niño Southern Oscillation (ENSO) (Mason and Jury 1997; Reason et al. 2000; Washington and Preston 2006; Philippon et al. 2012). Over the winter rainfall region of South Africa, interannual rainfall variability is linked to the geographical location of storm tracks, i.e. cold fronts, which are in turn linked to the SAM and more recently ascribed in the literature to ENSO as well. Wet winters are associated with the negative phase of the SAM (Reason and Rouault 2005) as well as with El Niño (Philippon et al. 2012) that cause storm tracks to be located further towards the equator, resulting in wet conditions (Reason and Rouault 2005; Philippon et al. 2012). ENSO is also linked to rainfall variability over the summer rainfall region, in particular mid-summer (Landman and Beraki 2012). Here, El Niño events are usually associated with below-normal rainfall and the less frequent occurrence of tropical-temperate troughs (e.g. Tozuka et al. 2014). However, the association between ENSO and the occurrence of tropical-temperate troughs is non-linear, as wet seasons do not necessarily experience more tropical-temperate troughs (Hart 2012). Our current understanding of rainfall variability over the Cape south coast region is based on very few studies (Jury and Levey 1993; Weldon and Reason 2014). A study that included part of the eastern half of the Cape south coast and that considered only the months of March and October, suggested qualitatively that COLs and ridging high pressure systems play a part in interannual rainfall variability by implication that the occurrence of these systems are disrupted during dry years (Jury and Levey 1993). In a more recent study, the association between anomalous rainfall years, ENSO and COLs was investigated (Weldon and Reason 2014). ENSO also seems to play a part in interannual rainfall variability over the Cape south coast via its association with the occurrence of COLs. Mature phase La Niña years are usually wet and accompanied by a higher frequency of COLs (Weldon and Reason 2014) from late spring to early autumn (Favre et al. 2013). Here, as with the association between tropical-temperate trough occurrence and ENSO, the association between COL frequency and ENSO is non-linear. Dry years are associated with a lower frequency of COLs, but without an ENSO association. The link between ENSO and rainfall variability over the Cape south coast seems mostly to be restricted to the association between increased COL frequency during the spring to autumn months of La Niña years, as other rainfall attributes such as monthly rainfall totals and monthly heavy rain event frequencies show unstable and weak correlations with the Niño 3.4 index (Weldon and Reason 2014). A stronger link is
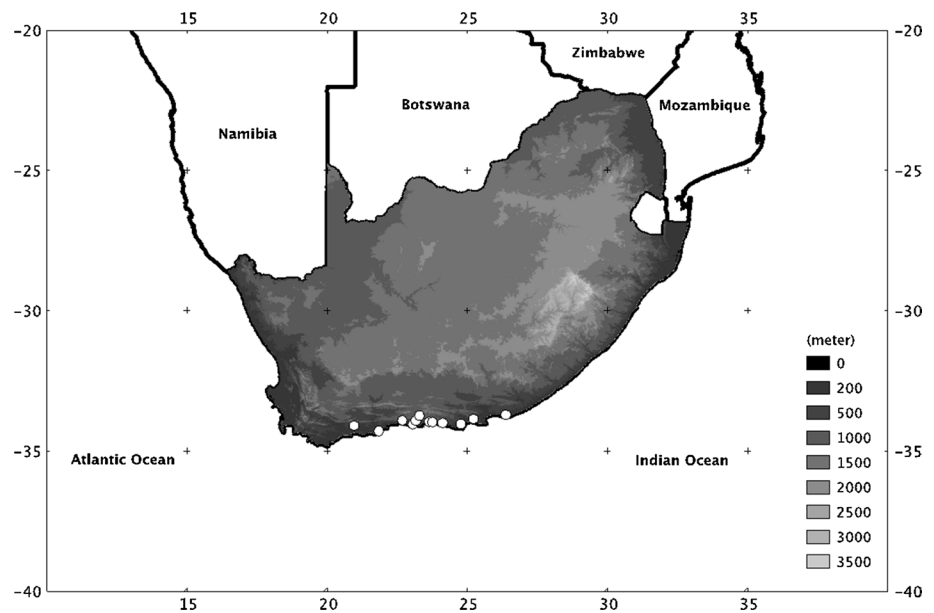
observed between wet-day frequency and the Niño 3.4 index (negative correlation) for December and January (Weldon and Reason 2014), the time of year when the impact of ENSO on rainfall over the summer rainfall region of South Africa is the strongest (Landman and Beraki 2012).

In this study, interannual variability in seasonal rainfall over the Cape south coast is investigated within the context of the high frequency variability of synoptic types, i.e. intraseasonal variability. The frequency of occurrence of the different synoptic types is therefore derived from daily circulation data and subsequently associated with anomalous rainfall on the seasonal time scales. Of specific interest are the regional features of rain-producing weather systems associated with rainfall variability. The aim of this study is to identify the specific configurations of the different synoptic types that are potentially linked to the interannual variability of seasonal rainfall, with the potential to apply the gained knowledge to application forecasts of intraseasonal variability. This aim requires the investigation of the potential link between the occurrence of COLs and rainfall variability as well, given the high impact rainfall events that can occur in association with COLs. Also, with the known ENSO association over the region (Weldon and Reason 2014) as well as the ENSO and SAM relationships over the winter (Reason and Rouault 2005; Philippon et al. 2012) and summer (van Heerden et al. 1988; Pohl et al. 2010; Malherbe et al. 2014a) rainfall regions, the potential association of these climate modes with the intraseasonal occurrence of synoptic regimes is explored.

2 Data and methodology

2.1 Rainfall data

Daily rainfall data for the 33-year period from 1979 to 2011 from 12 weather stations of the South African Weather Service (SAWS) over the Cape south coast were considered in this study (Fig. 1). These 12 stations were chosen based on their availability (defined here as the presence of data on more than 90 % of the days in a specific month) and quality. Extreme and missing value tests were employed as data quality measures. Values that did not comply with these tests were replaced by estimated values derived from neighbouring stations. Seasonal rainfall totals for each station were calculated from this complete daily rainfall dataset. The seasons considered here are austral summer, autumn, winter and spring, comprising December to February (DJF), March to May (MAM), June to August (JJA) and September to November (SON) respectively. The seasonal rainfall totals were spatially averaged and then ranked in order to identify years of above-normal, near-normal and below-normal seasonal rainfall. Thirty-two years of seasonal rainfall totals were considered for each of the four seasons. For each of the seasons the upper-most 10 totals were used to define above-normal rainfall, the 10 lower-most totals define below-normal rainfall and near-normal rainfall is defined by the remaining 12 rainfall totals. The rainfall station data were used to quantify the contribution of COLs to seasonal rainfall totals in order to investigate the role of COLs in interannual variability of seasonal rainfall.

2.2 Classification of synoptic types and identification of COLs

The focus of this paper is to relate interannual variability in seasonal rainfall to synoptic types. Synoptic types that represent archetypical atmospheric states were classified by application of the SOM technique (Kohonen 2001). A 35-node SOM was developed from daily sea-level pressure (SLP) anomaly fields derived from the daily average SLP fields from the National Centers for Environmental Prediction (NCEP) reanalysis data (Kalnay et al. 1996) for the region bounded by 45°S–32.5°S and 10°E–40°E. The SLP anomaly fields are effectively gradient fields that drive circulation (Schuenemann et al. 2009). Over the Cape south coast, low-level circulation is important to facilitate moisture advection from the surrounding ocean (Rouault et al. 2002; Singleton and Reason 2006, 2007a)—hence the choice of the SOM domain. A full description on the development of the SLP anomaly SOM can be found in Engelbrecht et al. (2015). In this paper, the composite maps of the 850 hPa geopotential height fields based on the SLP anomaly SOM are employed to represent the archetypical atmospheric states. The decision to employ the 850 hPa geopotential height fields to present the synoptic types in this study is to allow for presenting the synoptic types over a domain extending further northwards. The 850 hPa pressure level takes the typical height of 1500 m of the South African plateau into consideration. The presentation of the synoptic types over a domain that includes a larger part of the subcontinent can complement the description of the synoptic types as the circulation over South Africa and surrounding oceans normally consist of segments of several circulation types. It can be noted that the synoptic types identified by the SLP anomaly SOM and those represented by the 850 hPa geopotential height composite maps over the larger domain, are consistent as the 850 hPa composite maps are derived from the daily entries in each node of the SLP anomaly SOM.

NCEP reanalysis data (Kalnay et al. 1996) are utilized to identify and track COLs over the period 1979–2011. COLs have a typical length scale of 1000 km (Singleton and Reason 2007b) and are therefore well resolved by the 2.5° resolution of the NCEP data. A COL is defined as a cold cored closed-low at 500 hPa that is displaced from the westerly wind regime (Favre et al. 2012). The daily-average geopotential height and temperature fields at 500 hPa are utilized for identifying and tracking COLs in the domain bounded by 40°S–20°S and 10°E–40°E. All the COLs that occurred for at least 24-h over this domain are considered in this study. Firstly, closed-lows are identified by locating geopotential minima in a procedure where the geopotential at each grid point is compared to the geopotential values of the square of eight surrounding grid points on the latitude

longitude grid. After closed-lows have been identified in the time series of 500 hPa geopotential fields, tracks are constructed by identifying the geopotential minima at time step $t + 1$ nearest to the geopotential minima at time step t. The distance between the closed-lows at time step t and time step $t + 1$ needs to be <1000 km in order to secure a sound mean daily speed of the potential COL. The mean daily speed of a COL in the South African region does not exceed 42 km/h (Favre et al. 2012). Any geopotential minima can only be used in a single track. From this closed-low track dataset, tests described in Favre et al. (2012) to ensure that tracks are of extra-tropical origin, are detached from the westerlies and possess a cold-core are employed.

Rainfall associated with cold-cored systems occurs mainly some hundreds of kilometres to the northeast, east and southeast of the centres of these systems. From the constructed COL dataset for the period 1979–2011, all the COLs that occurred west of 32.5°E, following Favre et al. (2013), were considered to be potentially responsible for rainfall over the region. Such COLs associated with rainfall over the region, at least at a single station, were defined as rainfall producing COLs.

2.3 Grouping of similar synoptic types into main circulation types

The synoptic types identified by the SOM consist of various configurations of the main circulation types. Each of the SOM nodes is classified into one of the main circulation types—following the grouping performed in Engelbrecht et al. (2015). These groups represent circulation types representative of troughs southwest of the subcontinent, troughs southeast of the subcontinent, ridging high pressure systems, ridges east/southeast of the subcontinent, tropical-temperate troughs and weak synoptic flow. The groups of synoptic types used here fall within the subdivisions of circulation types (anticyclones, cyclones, ridges, troughs and zonal flow) identified and described by Taljaard (1995). Troughs southwest or southeast of the subcontinent fall within the west wind trough circulation type (e.g. Taljaard 1995), with the distinguishing factor being the position of the westerly trough relative to the subcontinent. Cold fronts, occurring during winter and summer as well as leader fronts, a winter circulation type, typically fall within these two groups while ridging high pressure systems and ridges east/southeast of the subcontinent are variations of ridges as described by Taljaard (1995). Tropical-temperate troughs, although part of the trough family, are considered separately as these systems are captured explicitly in the SOM (e.g. Tozuka et al. 2014) and due to its importance with regard to rainfall contribution over South Africa (Harrison 1984; Washington and Todd 1999; Hart et al. 2013). COLs are part of the cyclone/low pressure family (Taljaard

1995) and co-occur with ridging high pressure systems (Katzfey and McInnes 1996; Favre et al. 2012; Engelbrecht et al. 2015) and tropical-temperate troughs (Hart et al. 2013; Engelbrecht et al. 2015). However, due to the infrequent occurrence of COLs (Engelbrecht et al. 2015), these systems are difficult to explicitly be captured in the SOM. COLs are therefore considered with ridging high pressure systems and tropical-temperate troughs in the analysis presented in this paper, unless where it is indicated that COLs are considered explicitly as identified by the objective COL identification and tracking algorithm (see Sect. 2.2). The group of similar synoptic types termed weak synoptic flow is similar to the zonal flow circulation type identified by Taljaard (1995). However, a difference may be that the circulation type zonal flow described by Taljaard (1995) can be associated with weak or tight pressure gradients, whereas the circulation type weak synoptic flow in this study is defined to be characterized by weak pressure gradients over the Cape south coast region.

Classification of the synoptic types into groups is feasible by visual inspection of the 850 hPa geopotential height node composites (typically as would be performed by an experienced weather forecaster), but introduces the challenge of objectivity due to the circulation over the study domain not normally characterized by a single circulation type. Classification of the synoptic types into groups representative of troughs southwest of the subcontinent, troughs southeast of the subcontinent, ridging high pressure systems, ridges east/southeast of the subcontinent, tropical-temperate troughs and weak synoptic flow was therefore achieved by careful consideration of the SOM node anomaly fields (850 hPa geopotential height composites) relative to climatology (not shown) and a hierarchical clustering method, Ward's minimum variance method (Wilks 2011). Ward's method was applied to the SOM nodes based on the SLP anomaly fields to aid in grouping of the synoptic types into the main circulation types.

2.4 Large-scale climate modes

The Oceanic Niño Index (ONI) is obtained for DJF, MAM, JJA and SON for 1979–2011 (32 DJF seasons and 33 MAM, JJA and SON seasons each) from the Climate Prediction Center (CPC) (www.cpc.ncep/noaa.gov/products/analysis_monitoring/ensostuff/ensoyears.shtml). The ONI is a 3-month running mean of ERSST.v3b (Smith et al. 2008) sea-surface temperature (SST) anomalies in the Niño 3.4 region (5°N–5°S, 120°W–170°W), and has already been used as an ENSO indicator for southern African variability and predictability studies (Landman et al. 2009, 2012). Monthly SAM (Mo 2000) index values are also obtained from CPC (www.cpc.ncep.noaa.gov/products/precip/CWlink/daily_ao_index/monthly.aao.index.b79.

current.ascii.table), and are used to derive the SAM index for DJF, MAM, JJA and SON for 1979–2011.

An objective of the paper is to further our current understanding (Weldon and Reason 2014) of the ENSO link and rainfall variability over the Cape south coast. As ENSO and SAM are related (Gong et al. 2010; Fogt et al. 2011), the teleconnection investigation performed here included an analysis that aims to address the potential link between SAM and the occurrence of synoptic regimes.

In order to determine whether the climate modes, ENSO and SAM, are separately correlated with the occurrence of synoptic regimes for each of the seasons DJF, MAM, JJA and SON, a synoptic regime index is derived. This index considers the frequency distribution of synoptic regimes within the SOM space and was derived for each of the seasons (DJF, MAM, JJA and SON) from the pattern correlation between the interannual frequency distribution within the SOM space and a reference frequency distribution. The reference frequency distribution is represented by the average frequency distribution of the wet years for the particular season. In this manner, a unique time series is developed for each of the seasons, which are then utilized in the correlation analysis with ENSO and SAM.

3 Results

3.1 Seasonal cycle of synoptic types

The 850 hPa geopotential height node-averaged fields are shown in Fig. 2 while the seasonal cycle of each node expressed as the percentage occurrence is shown in Fig. 3. Nodes with a strong winter occurrence are observed in the bottom row of the SOM (nodes 1–6), while nodes occurring most frequently in summer are found in the top row (nodes 29–35). The nodes in the top row of the SOM also show a high frequency of occurrence during the transitional seasons, autumn and spring. However, the highest frequency of occurrence during autumn is found over the left-central part of the SOM (node 15) representative of a surface trough over the far western part of the country linking up with a westerly trough to the southwest of the subcontinent (Fig. 2). During spring, nodes located over the right-central part of the SOM (in particular node 21), representative of ridging high pressure systems, exhibit the highest frequency of occurrence. The various configurations of winter frontal systems are represented by nodes 1–6. Frontal systems without a pronounced winter occurrence, e.g. represented by nodes 8 and 9, are characterized by a weaker pressure gradient than frontal systems with a strong winter occurrence, e.g. nodes 1 and 2 (Fig. 2). The frontal systems characterized by stronger pressure gradients are the synoptic types contributing least to annual rainfall over the Cape

Fig. 2 Node-averaged 850 hPa heights of the 35-node SOM developed from daily SLP anomaly fields for the period 1979–2011
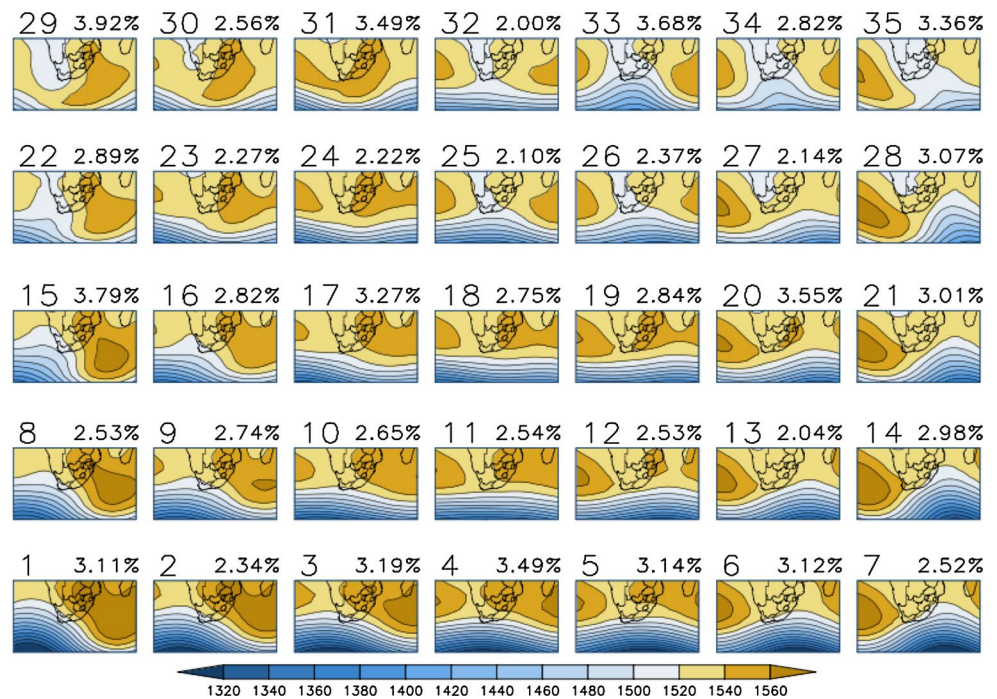
south coast (Engelbrecht et al. 2015), while these systems are the important rain-producing systems over the winter rainfall region (Lennard and Hegerl 2015). Ridging high pressure systems and tropical-temperate troughs, found in the top right part of the SOM (nodes 27, 28, 33, 34 and 35), are major contributors to annual rainfall over the Cape south coast (Engelbrecht et al. 2015). Noteworthy is that these systems sometimes co-occur with COLs (Engelbrecht et al. 2015). Nodes representative of synoptic types that occur throughout the year, but lacks evidence of a preferred season of occurrence, are found in the central part of the SOM (Fig. 3), and are in general insignificant with regard to annual rainfall contribution over the region (Engelbrecht et al. 2015). It is noteworthy that Ward's method provides results that are consistent with the grouping of synoptic types into a number of main synoptic types as described above. For example, nodes 28 and 35, indicative of ridging highs are grouped together by Ward's method. Similarly, nodes 33 and 34, indicative of tropical-temperate troughs, are grouped together.

3.2 Circulation anomalies during seasons of anomalous rainfall

Figure 4 shows the rainfall totals for 32 DJF (1979/1980–2010/2011), MAM (1980–2011), JJA (1980–2011) and SON (1980–2011) seasons. A similar analysis at annual time scales is not meaningful, because of a given year having the potential to be wet (or dry), for very different reasons. For example, a year with above-normal rainfall

induced by a wet SON will exhibit different synoptic frequencies than a wet year associated with a wet JJA.

Circulation anomalies associated with wet and dry seasons are presented in terms of the frequency of synoptic archetypes occurring during the relevant wet and dry seasons. Circulation anomalies associated with the SOM-nodes for seasons of above-normal, near-normal and below-normal rainfall are calculated relative to the relevant long-term mean for each of the nodes and are expressed as a percentage change of the actual node value before the relevant individual seasons are averaged for the wet, normal and dry seasons (Fig. 5). Rainfall anomalies are presented by using two different anomaly metrics to aid in the interpretation of rainfall characteristics that occur during wet and dry seasons. Figure 6 shows the average rainfall anomalies (mm) relative to the climatological value of the actual node for the relevant wet, normal and dry seasons. Figure 7 shows the rainfall percentage associated with each SOM-node, averaged for seasons of above-normal, near-normal and below-normal rainfall. Evident from Fig. 5 is the contrasting frequency relative to the climatological frequency of synoptic archetypes that occur during seasons of above-normal (Fig. 5a, d, g, j) and below-normal (Fig. 5c, f, i, l) rainfall. Table 1 shows the Kendall's tau rank correlation between the 35 node frequencies associated with above-normal rainfall and the corresponding 35 frequencies associated with below-normal rainfall, for each of the four seasons. The contrasting frequency of occurrence of the synoptic archetypes during wet and dry DJF seasons is significant at the 95 % level of confidence (Kendall's tau
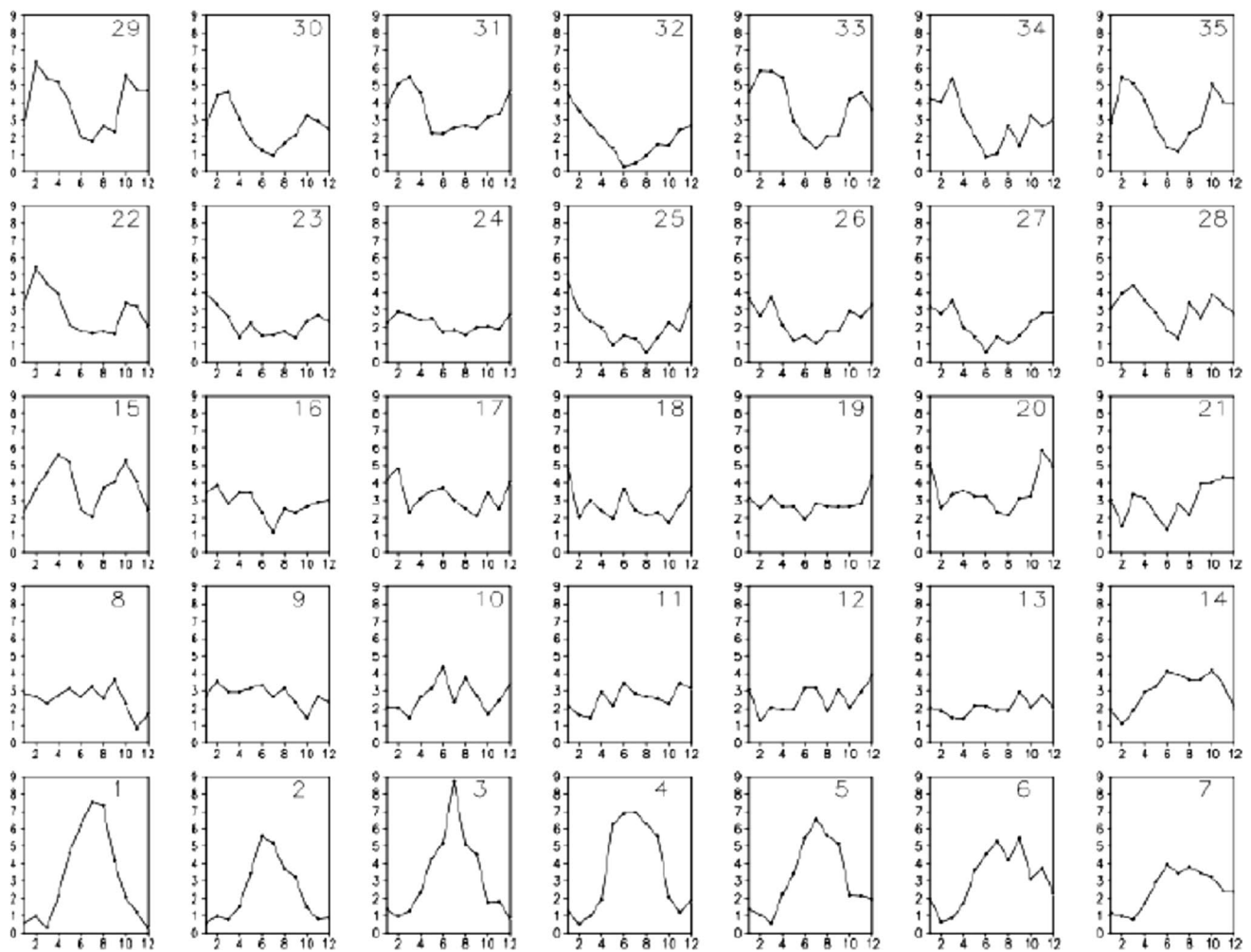
Fig. 3 Annual cycle (months indicated on the *x*-axis) of the percentage occurrence (*y*-axis) for the synoptic types identified by the SOM (*node number* indicated in the *top-right* of each panel)

rank correlation) while differences in the synoptic archetype frequencies between wet and dry MAM and JJA seasons are significant at the 90 and 99 % level of confidence (Kendall's tau rank correlation) respectively (Table 1). The Pearson product-moment correlation coefficients suggest for this relationship to be linear, in particular for JJA (not shown). Interesting to note is that such a reserved symmetry in terms of the frequency of synoptic archetypes does not exist for dry and wet SON seasons (Table 1), although synoptic archetype frequencies differ significantly between dry and normal SON seasons (not shown). The rainfall anomalies (Fig. 6) mirror the corresponding circulation anomalies (Fig. 5) with regard to the sign of the anomaly, illustrating the link between the total rainfall and the frequency of synoptic types, which suggests that the frequency of occurrence of these synoptic archetypes plays a role in determining whether seasons are dry/wet. The percentage rainfall associated with each node in the SOM

during wet and dry seasons (Fig. 7) reveals further that the nodes associated with rainfall are very similar during above-normal (Fig. 7a, d, g, j), near-normal (Fig. 7b, e, h, k) and below-normal (Fig. 7c, f, i, l) rainfall seasons. Circulation anomalies during seasons of near-normal rainfall are characterized by a mixture of circulation anomalies that also occur during wet and dry seasons.

Figure 8 shows the node-averaged meridional vertically integrated moisture flux for the SOM. The main rainfall-producing synoptic types found in the far right part of the SOM (e.g. nodes 14, 21 and 28) are associated with a vertically integrated northward moisture flux with the largest moisture flux located to the south of the subcontinent (Fig. 8). Other main rainfall-producing nodes (e.g. nodes 22, 29, 30, 33, 34 and 35) are characterized by a vertically integrated southward moisture flux in a northwest-southeast orientated band over the interior extending over the ocean southeast of the subcontinent in some of these nodes,
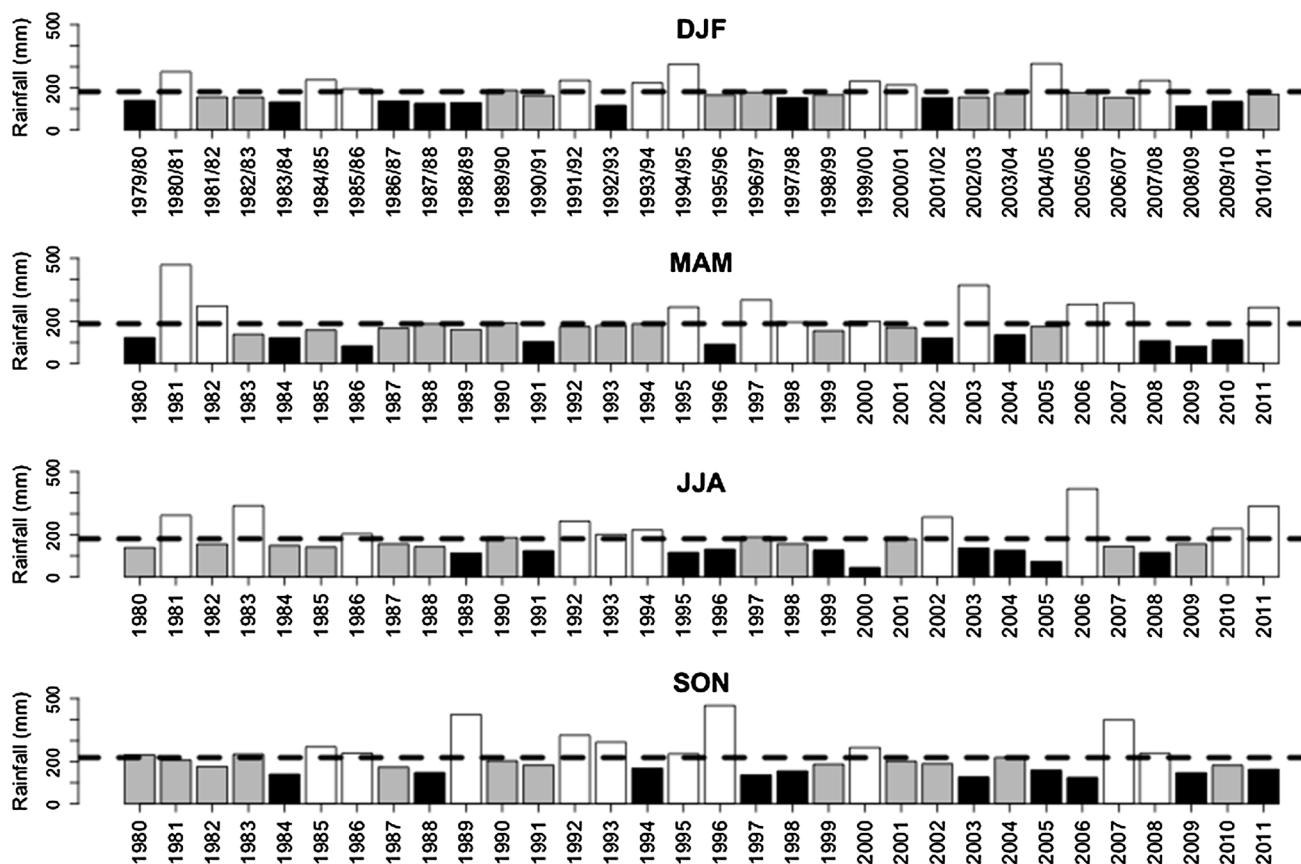
Fig. 4 The seasonal rainfall (mm) over the Cape south coast for 32 DJF, MAM, JJA and SON years over the period 1979–2011. The long-term mean rainfall for each season is indicated by a *black* *dashed line*. Seasons of above-normal, near-normal and below-normal rainfall are indicated by *white*, *grey* and *black* respectively

characteristic of cloud bands typical of summer (Todd et al. 2004; Hart et al. 2010, 2013; Tozuka et al. 2014). Vertical profiles of the meridional moisture flux over the Cape south coast, represented by the location at 35°S and 25°E, for wet and dry DJF, MAM, JJA and SON seasons, are shown in Fig. 9. For the purpose of visibility, vertical profiles for selected main rainfall-producing nodes, representative of these main rainfall-producing synoptic types, are shown. In general, three different moisture profiles are observed—moisture profiles characterized by a northward moisture flux (e.g. 28), a southward moisture flux (e.g. node 29) and profiles with a northward flux in the low-levels and a southward flux in the mid-levels (e.g. nodes 33 and 35). Considerable variation occurs in the latter case. For example, node 35 is characterized by a prominent northward low-level moisture flux during most seasons (Fig. 9), as may be expected from low-level ridging along the Cape south coast. Node 35 exhibits a more pronounced low-level northward moisture flux compared to node 33, being stronger and notably deeper, extending up to 775 hPa. This relatively strong northward moisture flux, overlayed by a southward moisture flux, is characteristic of convective

overturning (Taljaard 1996), also known as "undercutting" and can act as a trigger for convection. Node 33 represents a very different vertical moisture flux profile. Here a prominent southward flux is always present, especially in the mid-levels (700 hPa), as may be expected to occur in association with tropical-temperate troughs.

As expected, maximum moisture fluxes associated with each node occur mostly at the pressure level closest to sea level, 1000 hPa here, with the moisture being advected northwards. For example, during DJF, MAM and SON node 28 is associated with the maximum northward moisture flux while node 14, representative of a winter synoptic type (Fig. 3), is associated with the maximum northward moisture flux during JJA. The exception is synoptic types representative of node 29, characterized by a southward moisture flux with the maximum moisture flux occurring at pressure levels closest to the height of the plateau over the interior, being the strongest during MAM and SON (Fig. 9).

Moisture profiles during wet and dry seasons are quite similar, with wet seasons having a slightly stronger moisture flux, particularly evident for nodes 14 (JJA), 28
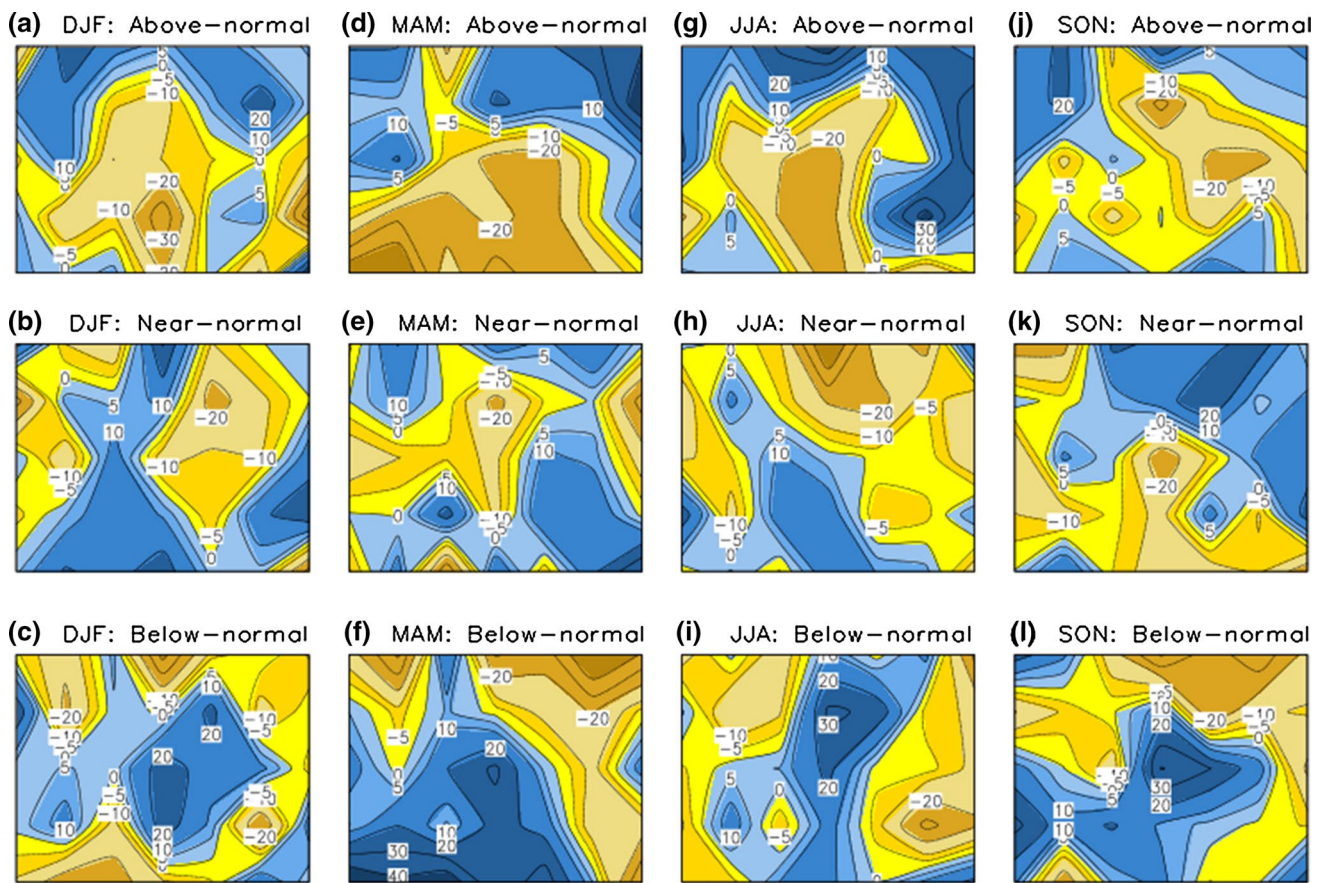
Fig. 5 Average circulation anomalies for seasons of above-normal (*top row*), near-normal (*middle row*) and below-normal (*bottom row*) rainfall as represented by the SOM-node frequency expressed as a percentage change for each of the nodes relative to the relevant long-term mean frequency of the relevant SOM-node. *Positive* (*negative*) anomalies are indicated by *blue shades* (*yellow shades*)

(MAM and SON) and 35 (SON). However, exceptions are observed for nodes 14 and 33 during DJF when moisture profiles of dry seasons have larger moisture fluxes than those of wet seasons. Node 14, representative of frontal systems, has a higher frequency of occurrence during dry seasons—explaining the larger moisture flux as confirmed in specific humidity profiles (data not shown). The larger moisture flux associated with node 33 during dry DJF seasons is due to stronger winds (not shown). Austral summer months during years of anomalous low rainfall over South Africa have been linked to the jet stream located anomalously equatorwards (Tennant and Reason 2005), implying stronger winds and cold fronts to have more equatorwards tracks.

Other contrasting circulation anomalies that are characteristic of below-normal and above-normal rainfall seasons occur over the central part of the SOM. These nodes are representative of weather systems associated with an equatorward pressure gradient (zonally orientated high pressure over the subcontinent and surrounding oceans with zonally orientated low pressure further southwards). An

equatorward pressure gradient (e.g. node 18) is not favourable for moisture advection over the Cape south coast. During above-normal (below-normal) rainfall seasons, an anomalously low (high) occurrence of weather systems characterized by this weak synoptic flow occurs.

3.3 Synoptic type rainfall and interannual variability of seasonal rainfall

Climatological seasonal rainfall totals over the Cape south coast are very similar (Table 2). Rainfall-producing synoptic types with an occurrence throughout the year includes ridging high pressure systems from the southwest and COLs while the contribution by tropical-temperate troughs and frontal systems peak during October to April and May to August respectively (Engelbrecht et al. 2015). In the case of ridging high pressure systems, seasonality is observed in the preferred configuration of this synoptic type that contributes to rainfall. For example, ridging high pressure systems from the southwest represented by nodes 7 and 14 are characteristic of winter, while nodes 20, 27
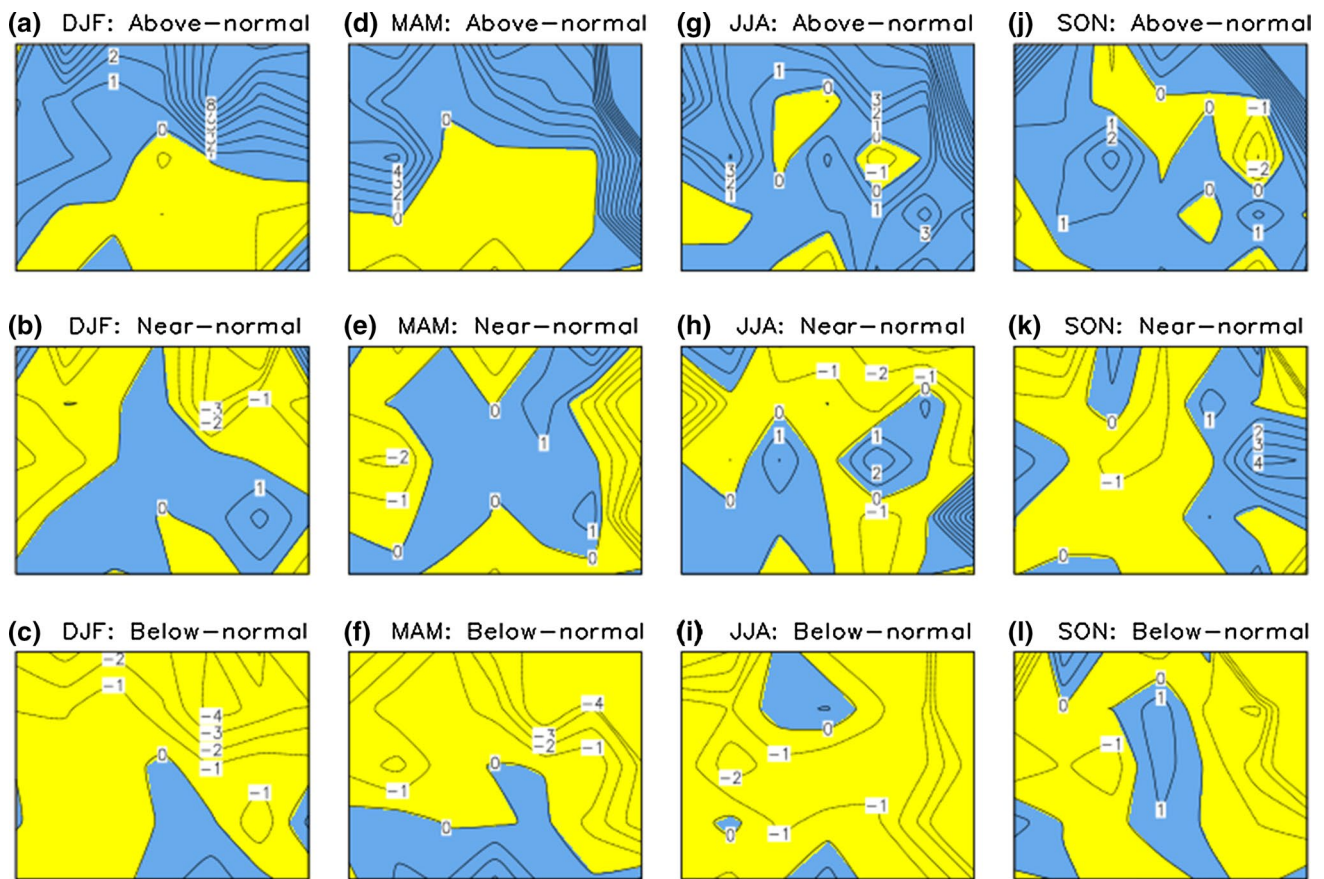
Fig. 6 Average rainfall anomalies (mm) for seasons of above-normal (*top row*), near-normal (*middle row*) and below-normal (*bottom row*) rainfall as represented by the rainfall associated with each of the nodes relative to the relevant long-term mean rainfall of the relevant SOM-node. *Positive* (*negative*) anomalies are indicated in *blue* (*yellow*)

and 35 exhibit summer peaks in their occurrence (Fig. 3). An objective of this paper is to identify important synoptic types and/or configurations within a specific synoptic type that are linked to interannual variability of seasonal rainfall over the Cape south coast. A direct approach to address this question is to test whether a significant positive correlation exists between the rainfall associated with the synoptic types and the total seasonal rainfall. It is firstly tested whether rainfall associated with nodes representative of a similar synoptic type collectively correlate with seasonal rainfall totals.

During DJF and MAM, rainfall associated with ridging high pressure systems from the southwest, ridges situated east of the subcontinent and tropical-temperate troughs (Table 3) exhibit a significant positive rank correlation with the respective seasonal rainfall totals, suggesting that these synoptic types are linked to interannual variability of DJF and MAM rainfall. During JJA and SON, rainfall associated with ridging high pressure systems from the southwest and ridges situated east of the subcontinent exhibit a significant positive rank correlation

with JJA and SON rainfall totals respectively (Table 3). Ridging high pressure systems from the southwest seem to have the strongest link to interannual variability of seasonal rainfall—significant at the 99 % level of confidence during DJF, MAM, JJA and SON, followed by ridges situated east of the subcontinent (Table 3). For the latter, the link to interannual variability seems stronger during DJF and MAM compared to JJA and SON. Pearson product-moment correlation coefficients indicate that this relationship is linear (not shown). Ridging high pressure systems from the southwest show the strongest linear relationship with interannual variability of seasonal rainfall. It may be noted that the maximum COL occurrence co-occurs with nodes within the groups representing ridging high pressure systems from the southwest (Fig. 2, node 35) and ridges situated east of the subcontinent (Fig. 2, node 29) (Engelbrecht et al. 2015). This is likely to influence the positive correlation of these groups with seasonal rainfall totals as COLs are associated with heavy rainfall events (Rouault et al. 2002; Singleton and Reason 2006, 2007a).
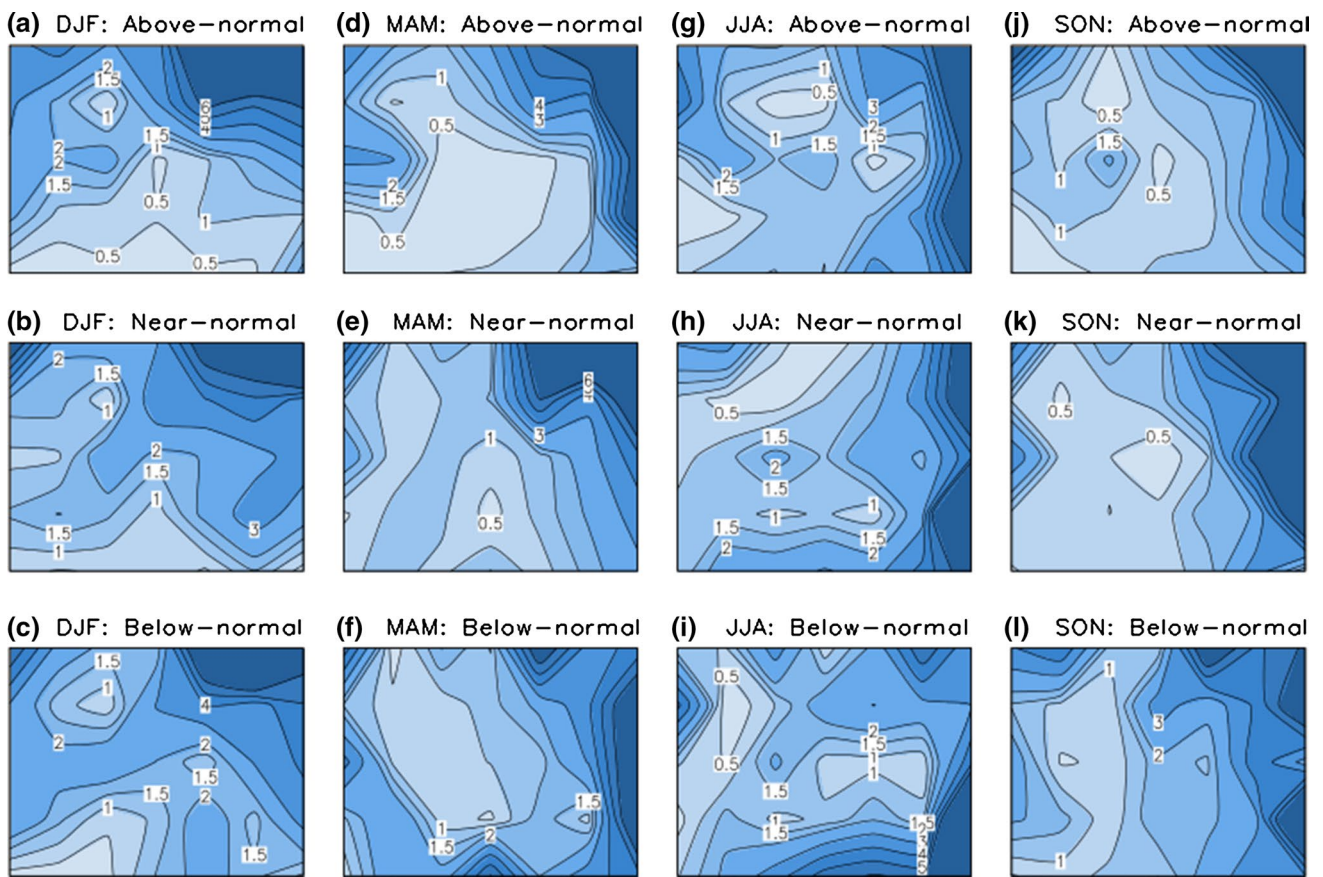
Fig. 7 Average percentage of rainfall for the SOM-nodes associated with seasons of above-normal (*top row*), near-normal (*middle row*) and below-normal (*bottom row*) rainfall

Table 1 Kendall's tau rank correlation between the frequency of synoptic archetypes during seasons of above-normal versus seasons of below-normal rainfall (see Fig. 5)

| DJF	MAM	JJA	SON
−0.26**	−0.208*	−0.415***	−0.0605

* 90 % level of confidence, ** 95 % level of confidence, *** 99 % level of confidence

The various configurations within the grouped synoptic types (represented by the individual nodes shown in Fig. 2), represent variations of attributes such as geographical and seasonal location, intensity and some structural features. In an attempt to highlight or isolate what specific configuration within a synoptic type is the preferred driver of interannual variability of seasonal rainfall, the seasonal rainfall associated with the individual nodes was also correlated with seasonal rainfall totals (Table 4). Noteworthy, is the presence of two specific configurations of ridging high pressure systems from the southwest, those with the most southward located axis (Fig. 2, nodes 28 and 35), that are correlated with rainfall totals for DJF, MAM, JJA

and SON. Ridging high pressure systems from the southwest representative of nodes 28 and 35 are suggested to be a driver of interannual variability of SON rainfall in particular with correlations significant at the 99 % level of confidence (Table 4). In the case of the tropical-temperate troughs, a significant correlation with DJF, MAM and SON rainfall totals exists. During DJF, rainfall associated with tropical-temperate troughs with the smallest node-averaged zonal wind component over and to the south of the country (nodes 32) are correlated to DJF rainfall totals, consistent with the jet stream that is located further poleward during years of above-normal rainfall over the summer rainfall region and hence weaker winds (Tennant and Reason 2005). During MAM and SON other configurations of tropical-temperate troughs are linked to interannual variability of seasonal rainfall, illustrating the seasonality that can occur within a specific group of synoptic types.

COLs contribute to 16 % of annual rainfall totals, co-occurring with ridging high pressure systems and tropical-temperate troughs (Engelbrecht et al. 2015). The nature of COLs to cause high impact rainfall events that have the ability to produce 24-h rainfall totals that exceed the

Fig. 8 Node-averaged meridional vertically integrated moisture flux (g m^{-1} s^{-1})
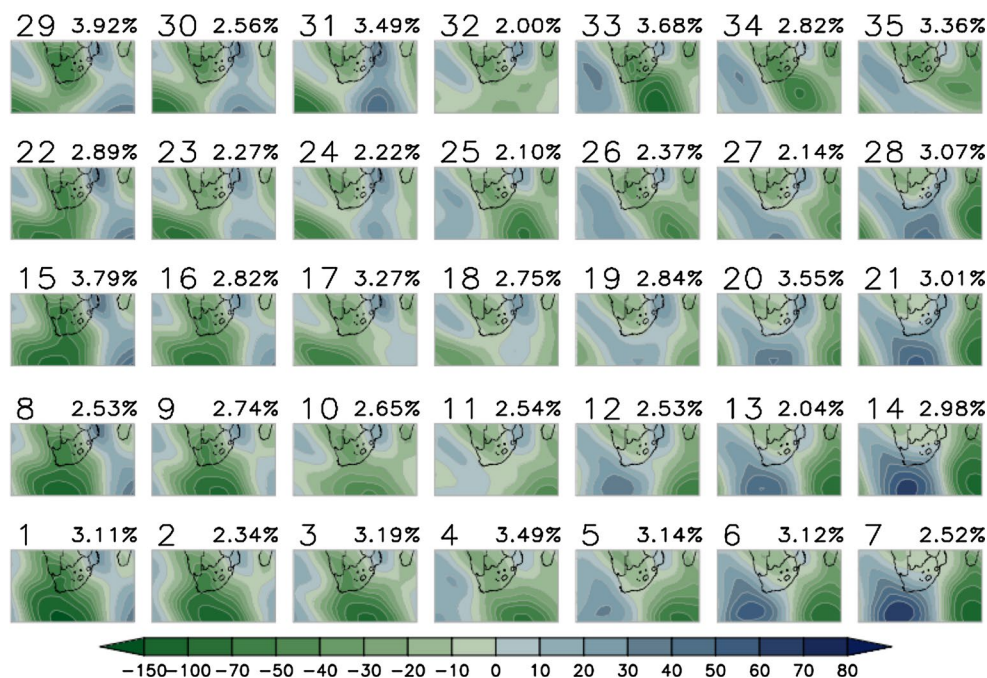
relevant climatological monthly rainfall (Singleton and Reason 2006, 2007a; Muller et al. 2008), warrants the consideration of a linkage between COL-induced rainfall and interannual variability in seasonal rainfall. Mean seasonal rainfall totals attributed to COLs are of comparable magnitude for MAM, JJA and SON with mean seasonal total rainfall during DJF only half or less of any of the other seasons (Table 5). Over South Africa COLs occur most frequently during MAM (31 %), followed by JJA (29 %), SON (22 %) and DJF (18 %) (Table 5), similar to COL seasonal frequencies from Singleton and Reason (2007b) and Favre et al. (2013). The relationship between the frequency of COLs and COL-induced rainfall is not linear. Although spring (SON) has a lower frequency of COLs than autumn (MAM) and winter (JJA), it is the season when the highest percentage of COLs is associated with rainfall over the Cape south coast. Spring, when defined as October–November–December (OND), is also the season when COL-induced rainfall over South Africa is on average widespread (Favre et al. 2013). During winter (JJA), the mean seasonal rainfall attributed to COLs over the Cape south coast is a maximum (38 mm) (Table 5). Favre et al. (2013) also identified winter [defined as July–August–September (JAS)] to be the season with the largest contribution to annual COL rainfall. South Africa on average, however, receives the largest contribution to annual COL rainfall during OND (Favre et al. 2013).

The influence of rainfall associated with COLs on seasonal rainfall totals is shown in Fig. 10. A weak and non-significant correlation exists for summer (DJF), the season with the lowest mean frequency of COLs and COL-associated rainfall. Autumn (MAM) and winter (JJA) have the highest and most significant (99 % level of confidence) correlation between COL-associated seasonal rainfall totals and all seasonal rainfall totals. A weak but significant correlation exists for spring (SON) which may be attributed to ridging high pressure systems that contribute largely to October rainfall, the month observed with the highest area-averaged monthly rainfall totals along the Cape south coast (Engelbrecht et al. 2015). The Pearson product-moment correlation coefficients indicate that the relationship between COLs and interannual rainfall variability is linear, in particular for JJA and MAM (not shown). Even though the frequency of occurrence of COLs is low, as illustrated by the absence of a node dedicated only to COLs in the SOM, COLs can have a notable impact on seasonal rainfall totals (e.g. JJA 2006, Fig. 10)—an indication of the intensity of COLs.

The geographical location of COLs during wet and dry seasons exhibits different regions of preferred occurrence (Fig. 11). The mean COL frequency anomaly for wet DJF seasons is characterized by COLs most frequently located over the western part of the Northern Cape and Southwestern Cape. During MAM, JJA and SON wet seasons are in general characterized by an increase in the frequency of COLs occurring countrywide. Noteworthy are areas of increased COL activity during wet seasons just off the Cape south coast and over the interior to the northwest of the Cape
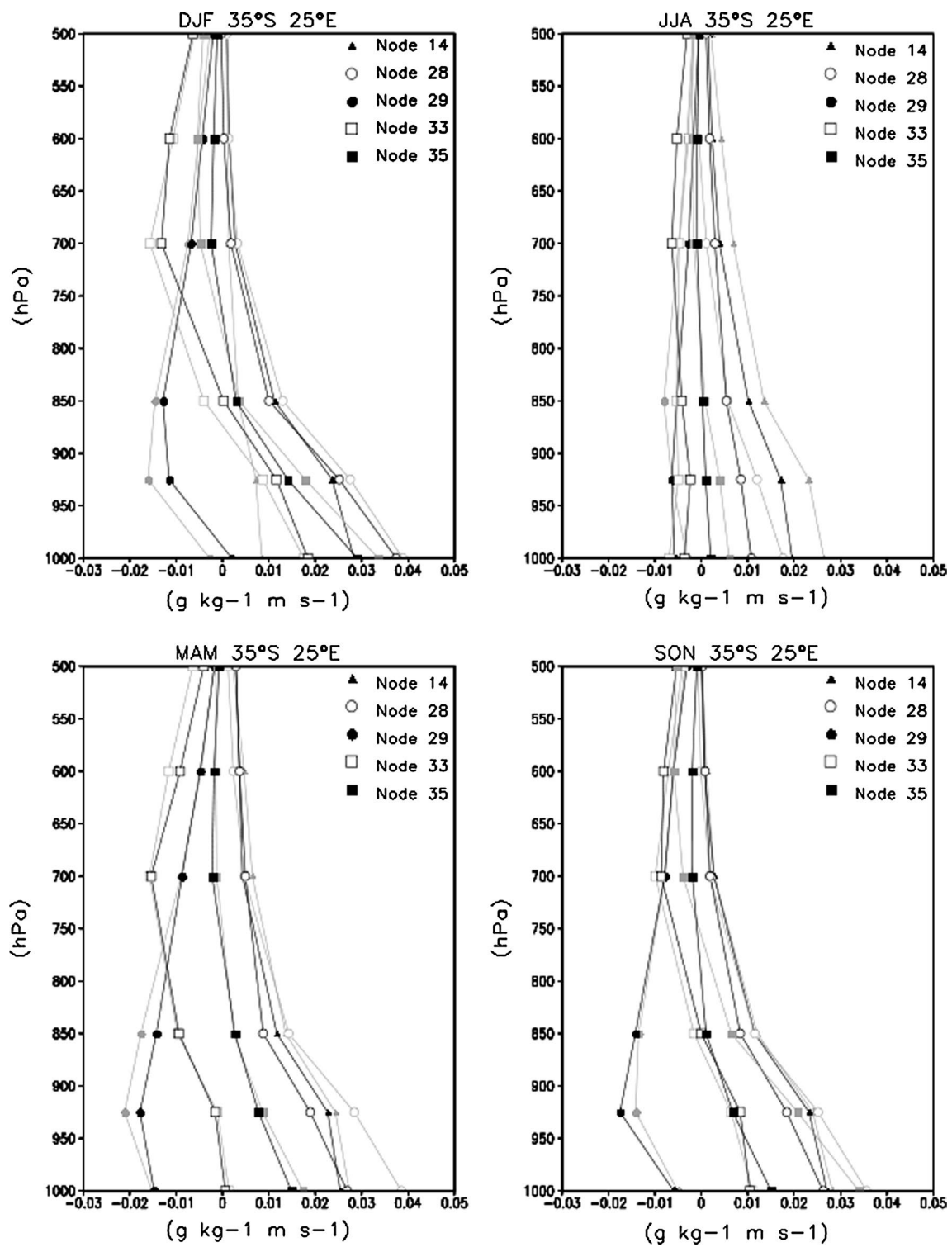
Fig. 9 Vertical profile of the meridional moisture flux (g kg^{-1} m s^{-1}) at 35°S and 25°E for wet (*grey*) and dry (*black*) DJF, MAM, JJA and SON years

south coast, consistent with increased mid-latitude cyclone system density associated with wet years (Weldon and Reason 2014). During seasons of below-normal rainfall, the aforementioned areas are generally characterized by a negative mean COL frequency anomaly, consistent with a pole-wards shift of storm tracks (Weldon and Reason 2014).

3.4 Large-scale climate modes

The SAM is significantly (99 % level of confidence) linked to the frequency distribution of nodes within the SOM space for the DJF (Fig. 12a) and MAM (Fig. 12b) seasons, while the relationship with ENSO is somewhat weaker (95 % level of confidence) and valid for DJF (Fig. 12c) and SON (Fig. 12d). This implies that for these seasons, given the predictability of ENSO (Barnston et al. 2011) and to a lesser extent SAM (Fogt et al. 2011; Gong et al. 2010) at the seasonal time scale, the skillful predictability of intraseasonal variability may be feasible (at the seasonal time scale). This relationship between the frequency distribution of nodes within the SOM space with SAM and ENSO respectively is linear according to Pearson product-moment correlation coefficients (not shown). Interesting to note is that the nature of the relationships between rainfall variability over the Cape south coast with ENSO and SAM respectively, are similar to that over the summer rainfall region where the positive (negative) phase of SAM (ENSO) is positively linked to rainfall. Over the winter

Table 5 Climatological seasonal statistics for COL induced rainfall in mm (second column), percentage of COL occurrences over South Africa (third column) and percentage of COLs that produce rainfall over the Cape south coast (fourth column)

Attribute	Long-term average seasonal COL rain (mm)	Long-term average seasonal COL distribution over South Africa (%)	Long-term average percentage of COLs over South Africa associated with rain over the Cape south coast (%)
DJF	15.3	18	56
MAM	33.8	31	61
JJA	38.4	29	63
SON	30.6	22	68

rainfall region of South Africa, the relationships between rainfall with ENSO and SAM are reversed. Over the Cape south coast wet-day frequency during early winter (June) is positively (negatively) linked to the positive (negative) phase of ENSO (Weldon and Reason 2014). Frontal systems representative of node 3 (Fig. 2) occur anomalously more frequent (the percentage change relative to climatology is 50 %) during El Niño events in June while they occur anomalously less frequent (the percentage change relative to climatology is −57 %) during La Nina events in June.
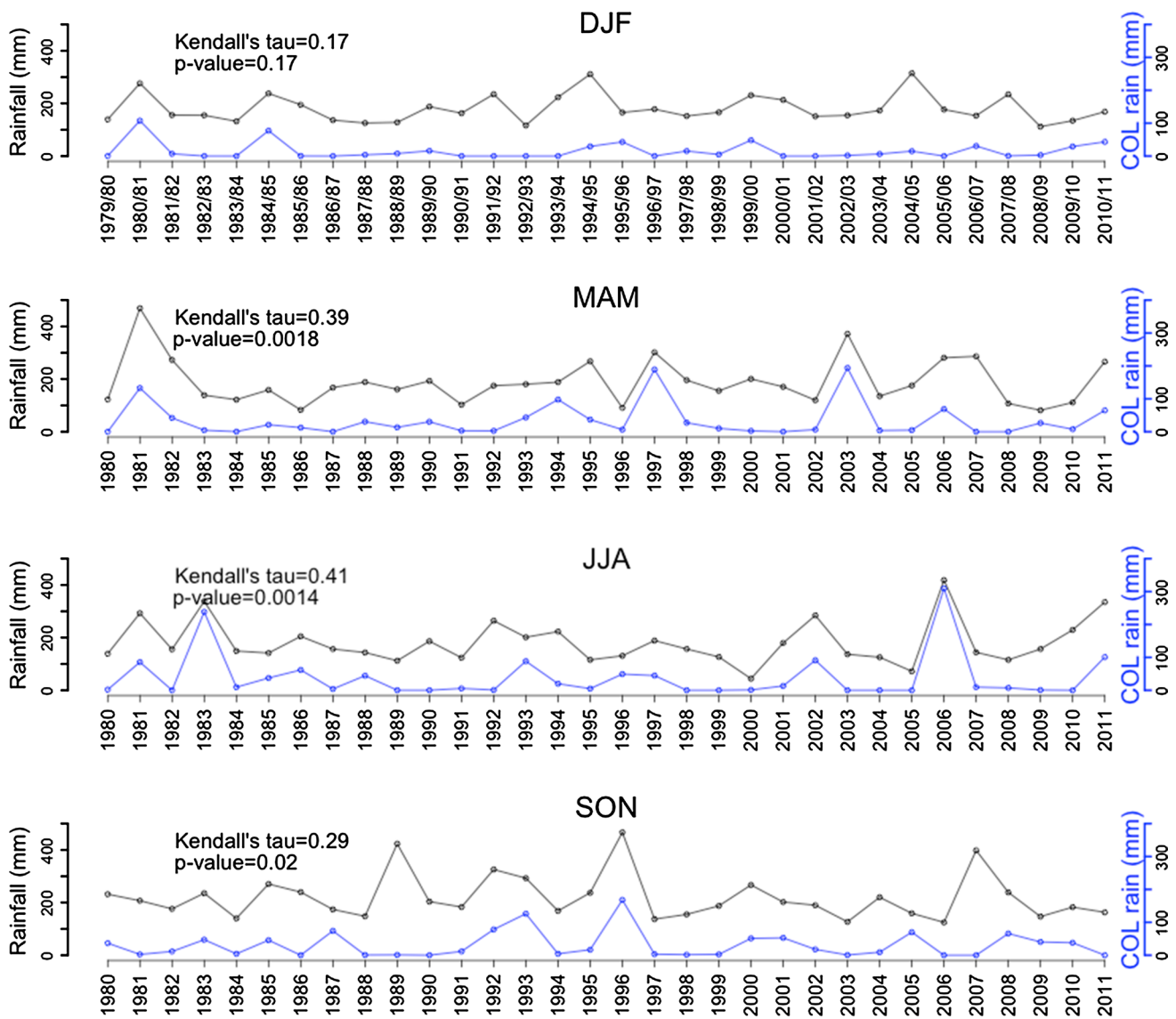
Table 2 Climatological seasonal rainfall totals (mm)

DJF	MAM	JJA	SON
181	189	181	219

Table 3 Kendall's tau rank correlation between circulation type seasonal rainfall (mm) and total seasonal rainfall (mm) over the period 1979–2011

Grouped synoptic types/main circulation types	Trough southwest	Trough southeast	Ridging high pressure	Ridge east	Tropical temperate trough	Weak synoptic flow
Nodes	1, 2, 3, 8, 9, 10	4, 5, 6, 11, 12	7, 13, 14, 20, 21, 27, 28, 35	17, 24, 29, 30, 31	15, 16, 22, 23, 25, 26, 32, 33, 34	18, 19
DJF	0.16	−0.19	0.42***	0.33***	0.26**	−0.006
MAM	−0.2	−0.14	0.69***	0.58***	0.32**	−0.06
JJA	0.16	0.07	0.58***	0.28**	0.19	−0.05
SON	−0.05	0.09	0.6***	0.24*	0.17	−0.09

* 90 % level of confidence, ** 95 % level of confidence, *** 99 % level of confidence

Table 4 Nodes for which the node-associated rainfall is significantly correlated with the seasonal rainfall totals over the period 1979 to 2011

Seasons	Nodes for which the node associated rainfall is significantly correlated with the seasonal rainfall totals
DJF	**27** (0.27**), **28** (0.23*), **32** (0.3**), **35** (0.22*)
MAM	**2** (−0.3**), **4** (−0.33***), **15** (0.25**), **16** (0.32**), **25** (0.24*), **27** (0.28**), **28** (0.22*), **30** (0.45***), **33** (0.26**), **34** (0.3**), **35** (0.32**)
JJA	**1** (0.25*), **2** (0.22*), **4** (−0.26**), **13** (0.3**), **21** (0.27**), **28** (0.44***), **29** (0.24*), **35** (0.25*)
SON	**8** (−0.29**), **16** (0.24*), **22** (0.22*), **28** (0.38***), **33** (0.24*), **35** (0.4***)

Node numbers are indicated in bold. Kendall's tau rank correlation and the significance level is indicated in brackets where * 90 % level of confidence, ** 95 % level of confidence and *** 99 % level of confidence

Fig. 10 Kendall's tau rank correlation between seasonal rainfall totals and the corresponding COL-induced rainfall totals

4 Discussion and conclusions

The association between interannual variability of seasonal rainfall over the Cape south coast of South Africa and synoptic types was investigated. The method of SOMs was employed to relate daily low-level circulation fields obtained from NCEP with daily area-averaged rainfall for the period 1979–2011. The daily circulation statistics obtained from the SOM analysis were employed to determine seasonal anomaly fields for each SOM node for seasons of above-normal, near-normal and below-normal rainfall totals. Similarly, rainfall anomalies relative to the climatological mean as well as the average percentage of rainfall associated with each node for seasons

of above-normal, near-normal and below-normal rainfall were determined. Analysis of synoptic type frequencies illustrated that, based on the frequency anomaly relative to the climatological frequency of the synoptic types, it is possible to distinguish anomalously wet DJF, MAM and JJA seasons from being anomalously dry. During SON, a discernable difference in the frequency of synoptic types is absent. During wet seasons, the main rainfall-producing synoptic types, representative of ridging high pressure systems and tropical-temperate troughs, occur more frequently. Noteworthy is that these synoptic types remain the main rain-producing synoptic types during dry seasons, but with an anomalously low frequency of occurrence. Being able to use synoptic type frequencies to discriminate between wet and dry seasons has potential implications for

Fig. 11 Geographic location of COLs (COL centre frequency per grid point) for DJF, MAM, JJA and SON seasons of above-normal (*top*) and below-normal (*bottom*) rainfall relative to the climatological mean of COL centre frequency per grid point. *Blue* (*yellow*) shading indicates a *positive* (*negative*) anomaly of COL centre frequency per grid point
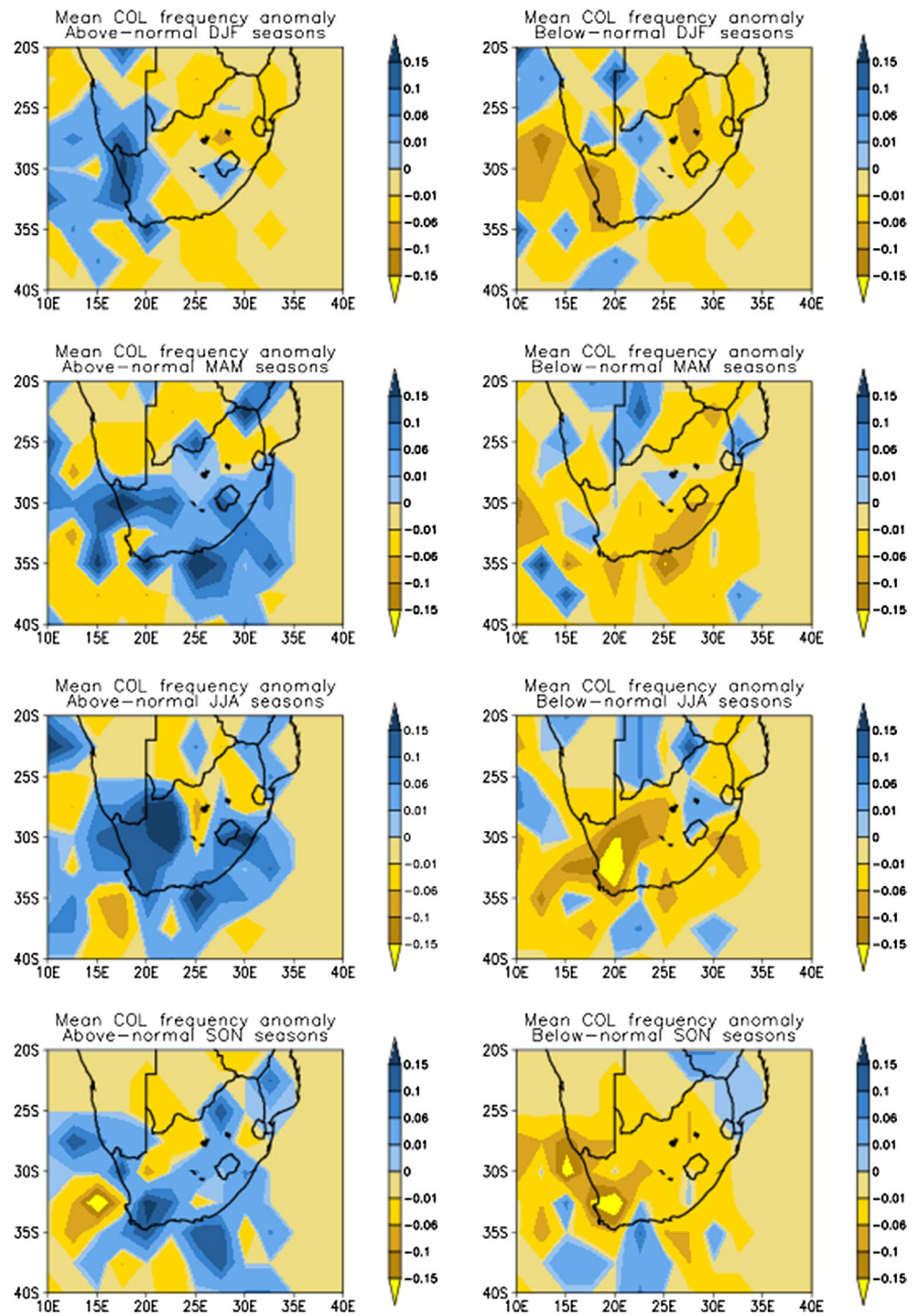
seasonal forecasting over the Cape south coast with regard to the confidence in discriminating between an above-normal or below-normal rainfall outlook. Skillful predictions of the differential synoptic type distributions for wet and dry seasons may be a requirement of skillful intra-seasonal rainfall prediction over the region.

Rainfall-producing westerly waves nearing the subcontinent are weakly linked to interannual variability of JJA rainfall, even though these systems are not regarded as the main rainfall-producing synoptic types over the Cape south coast. Indeed, during MAM and SON some configurations of westerly wave associated rain are negatively correlated with the respective seasonal rainfall totals. Rainfall associated with the main synoptic types representative of ridging high pressure systems and tropical-temperate troughs are linked to interannual variability of seasonal rainfall.
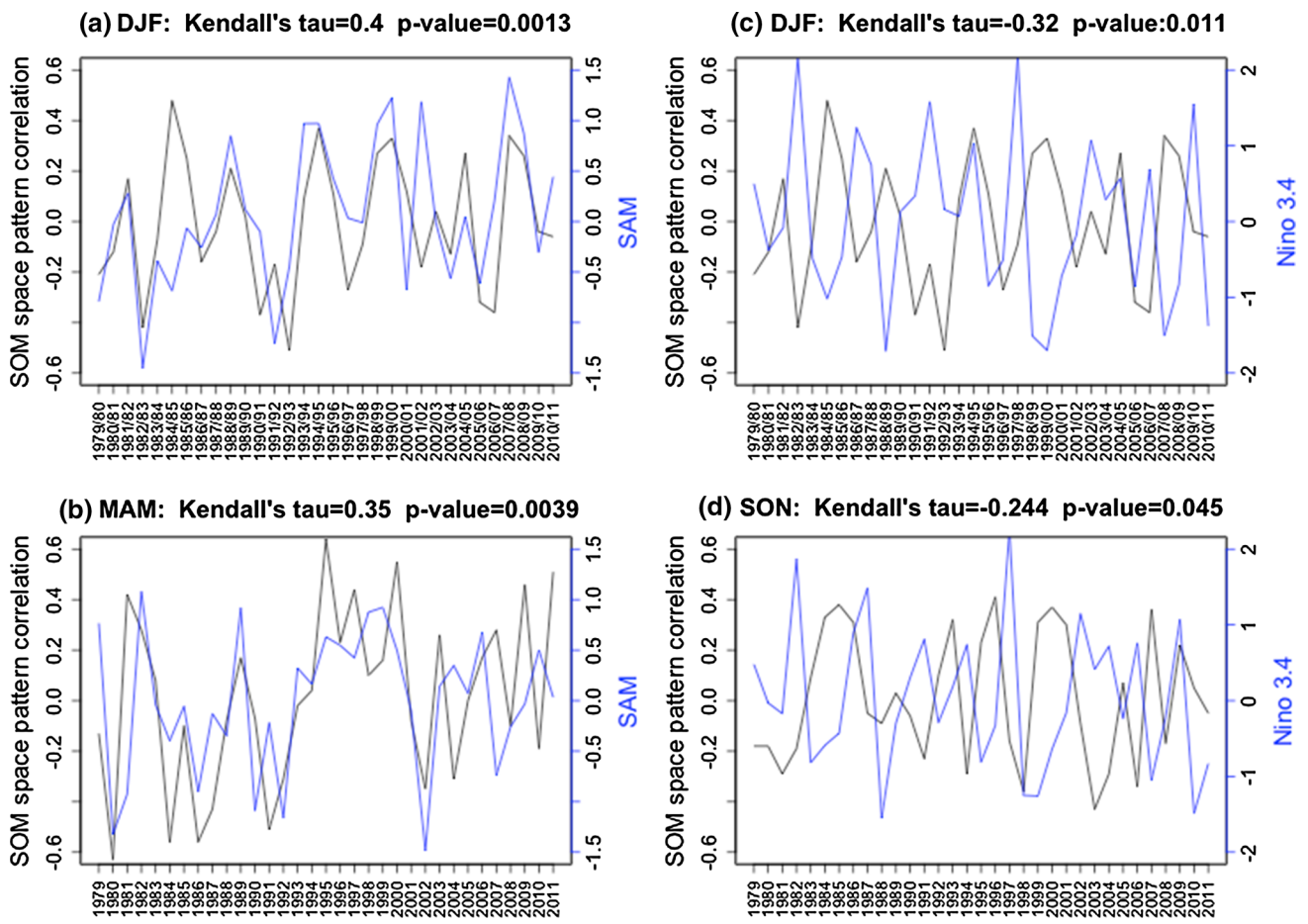
Fig. 12 Pattern correlation between the interannual frequency distribution of nodes within the SOM space and that of the average seasonal frequency distribution of nodes within the SOM space for the relevant wet season versus **a** the corresponding SAM index for DJF, **b** the corresponding SAM index for MAM, **c** the corresponding ONI for DJF and **d** the corresponding ONI for SON. The Kendall's tau values and level of significance are indicated in the respective *title bars*

A strong link is suggested for high pressure systems ridging from the southwest during DJF, MAM, JJA and SON while ridges east/southeast of the subcontinent and tropical-temperate troughs exhibit seasonality in its link to interannual variability of seasonal rainfall over the Cape south coast. Ridges east/southeast of the subcontinent exhibit a stronger link during DJF and MAM compared to JJA and SON while a link between tropical-temperate troughs is indicated to exist only during DJF and MAM. Specific configurations of ridging high pressure systems that are linked to interannual variability of seasonal rainfall, exhibit their ridging axis to be located further polewards (in particular nodes 28 and 35) than those not directly linked to interannual variability of seasonal rainfall. Both these nodes (28 and 35) are representative of weather systems with strong upper-air control. Node 35 is associated with the occurrence of COLs, while node 28 is associated with sharp upper-air troughs. The specific tropical-temperate trough configuration linked to interannual variability of DJF rainfall is suggestive of a slower moving tropical-temperate trough (node 32) with the zonal wind exhibiting similar characteristics to those of wet summers over the summer rainfall region of South Africa (Tennant and Reason 2005). The zonal wind characteristics associated with node 32 are in contrast to the mean circulation associated with wet winters over the winter rainfall region when an anomalously strong jet is found just upstream of the subcontinent (Reason and Rouault 2005) that has also been linked to El Niño conditions (Philippon et al. 2012). In general, this node (node 32) occurs mostly in La Niña years. The DJF seasons corresponding with the 10 DJF seasons of the highest occurrence of this node (node 32), display a preference for La Niña years as it consists of 5 La Niña years, 2 El Niño years and 3 neutral years.

A strong link is suggested between COL-induced rainfall and rainfall variability over the Cape south coast for MAM, JJA and SON, with the strongest link found for JJA. Winter is also the season when the mean

contribution by COLs to seasonal rainfall totals is the largest in the region (Favre et al. 2013; Engelbrecht et al. 2015). Regarding the geographical location of COLs, there seem to be distinct regions of preferred occurrence during wet and dry seasons, with anomalously more COLs located over the country during wet seasons, in particular over the southern and western parts.

Rainfall variability over the Cape south coast seems to be linked, as demonstrated by the frequency distribution of synoptic types within the SOM space, to the large-scale climate modes of ENSO and SAM. This link may be attributed to the association between ENSO and SAM (L'Heureux and Thompson 2006). The frequency distribution of nodes within the SOM space associated with wet seasons exhibits a statistically significantly positive correlation with the SAM during DJF and MAM, while this relationship associated with ENSO is negative (implying a positive relationship between rainfall and La Niña) and valid for DJF and SON. This result supports the state described by node 32, the slower moving tropical-temperate trough discussed above, contributing to rainfall variability and the potential role it has during La Niña events. Interesting to note though is that the seasons during which the ENSO association occurs over the region, coincide with spring to early autumn during which a positive association exists between COL occurrences and La Niña events (Favre et al. 2013). With rainfall variability over the Cape south coast linked to the large-scale climate drivers SAM and ENSO, as well as the occurrence of synoptic regimes during wet and dry seasons distinct with regard to their frequency and location within the SOM space, intraseasonal predictability applicable to the region seems feasible and needs to be explored further.

References

Barclay JJ, Jury MR, Landman W (1993) Climatological and structural differences between wet and dry troughs over Southern Africa in the early summer. Meteorol Atmos Phys 51:41–54

Barnston AG, Tippett MK, L'Heureux ML, Li S, DeWitt DG (2011) Skill of real-time seasonal ENSO model predictions during 2002–2011: is our capability increasing? Bull Am Meteorol Soc 93:631–651. doi:10.1175/BAMS-D-11-00111.1

Cook C, Reason CJC, Hewitson BC (2004) Wet and dry spells within particular wet and dry summers in the South African summer rainfall region. Clim Res 26:17–31

Crétat J, Richard Y, Pohl B, Rouault M, Reason C, Fauchereau N (2012) Recurrent daily rainfall patterns over South Africa and associated dynamics during the core of the austral summer. Int J Climatol 32:261–273. doi:10.1002/joc.2266

Engelbrecht CJ, Landman WA, Engelbrecht FA, Malherbe J (2015) A synoptic decomposition of rainfall over the Cape south coast of South Africa. Clim Dyn 44:2589–2607. doi:10.1007/s00382-014-2230-5

Fauchereau N, Pohl B, Reason CJC, Rouault M, Richard Y (2009) Recurrent daily OLR patterns in the southern Africa/Southwest Indian Ocean region, implications for South African rainfall and teleconnections. Clim Dyn 32:575–591

Favre A, Hewitson B, Tadross M, Lennard C, Cerezo-Mota R (2012) Relationships between cut-off lows and the semiannual and southern oscillations. Clim Dyn 38:1473–1487. doi:10.1007/s00382-011-1030-4

Favre A, Hewitson B, Lennard C, Cerezo-Mota R, Tadross M (2013) Cut-off lows in the South Africa region and their contribution to precipitation. Clim Dyn 41:2331–2351. doi:10.1007/s00382-012-1579-6

Fogt RL, Bromwich DH, Hines KM (2011) Understanding the SAM influence on the South Pacific ENSO teleconnection. Clim Dyn 36:1555–1576

Gong T, Feldstein SB, Luo D (2010) The impact of ENSO on wave breaking and Southern Annular Mode events. J Atmos Sci 67:2854–2870

Harrison MSJ (1984) A generalized classification of South African rain-bearing synoptic systems. Int J Climatol 4:547–560

Hart NCG (2012) Synoptic-scale rainfall patterns over southern Africa: scale-interactions with large-scale modes of variability. Unpublished PhD thesis

Hart NCG, Reason CJC, Fauchereau N (2010) Tropical–extratropical interactions over Southern Africa: three cases of heavy summer season rainfall. Mon Weather Rev 138:2608–2623

Hart NCG, Reason CJC, Fauchereau N (2013) Cloud bands over southern Africa: seasonality, contribution to rainfall variability and modulation by the MJO. Clim Dyn 42:1199–1212. doi:10.1007/s00382-012-1589-4

Holloway A, Fortune G, Zweig P, Barrett L, Benjamin A, Chasi V, de Waal J (2012) Eden and Central Karoo Drought Disaster 2009–2011; "The Scramble for Water." For the Provincial Disaster Management Centre, Western Cape by the Disaster Mitigation for Sustainable Livelihoods Programme, Department of Geography and Environmental Studies, Stellenbosch University

Jury MR, Levey K (1993) The climatology and characteristics of drought in the eastern Cape of South Africa. Int J Climatol 13:629–641

Jury MR, Pathack BMR, Sohn BJ (1992) Spatial structure and interannual variability of summer convection over southern Africa and the SW Indian Ocean. S Afr J Sci 88:275–280

Kalnay E, Kanamitsu M, Kistler R, Collins W, Deaven D, Gandin L, Iredell M, Saha S, White G, Woollen J, Zhu Y, Leetmaa A, Reynolds B, Chelliah M, Ebisuzaki W, Higgins W, Janowiak J, Mo KC, Ropelewski C, Wang J, Jenne R, Joseph D (1996) The NEP/NCAR 40-year reanalysis project. Bull Am Meteorol Soc 77:437–471

Katzfey JJ, McInnes KL (1996) GCM simulations of eastern Australia cutoff lows. J Clim 9:2337–2355

Kohonen T (2001) Self-organizing maps, 3rd edn. Springer, Berlin

L'Heureux ML, Thompson DWJ (2006) Observed relationships between the El Niño–Southern Oscillation and the extratropical zonal-mean circulation. J Clim 19:276–287

Landman WA, Beraki A (2012) Multi-model forecast skill for midsummer rainfall over southern Africa. Int J Climatol 32:303–314. doi:10.1002/joc.2273

Landman WA, Kgatuke MJ, Mbedzi M, Beraki A, Bartman A, du Piesanie A (2009) Performance comparison of some dynamical and empirical downscaling methods for South Africa from a seasonal climate modeling perspective. Int J Climatol 29:1535–1549. doi:10.1002/joc.1766

Landman WA, DeWitt D, Lee DE, Beraki A, Lötter D (2012) Seasonal rainfall prediction skill over South Africa: one-versus two-tiered forecasting systems. Weather Forecast 27:489–501

Lennard C, Hegerl G (2015) Relating changes in synoptic circulation to the surface rainfall response using self-organizing maps. Clim Dyn 44:861–879. doi:10.1007/s00382-014-2169-6

Malherbe J, Landman WA, Engelbrecht FA (2014a) The bi-decadal rainfall cycle, Southern Annular Mode and tropical cyclones over the Limpopo River Basin, southern Africa. Clim Dyn 42:3121–3138. doi:10.1007/s00382-013-2027-y

Malherbe J, Landman WA, Olivier C, Sakuma H, Luo J-J (2014b) Seasonal forecasts of the SINTEX-F coupled model applied to maize yield and streamflow estimates over north-eastern South Africa. Meteorol Appl 21:733–742. doi:10.1002/met.1402

Mason SJ, Jury MR (1997) Climatic variability and change over southern Africa: a reflection on underlying processes. Prog Phys Geogr 21:23–50

Mo KC (2000) Relationships between low-frequency variability in the southern Hemisphere and sea surface temperature anomalies. J Clim 13:3599–3610

Muller A, Reason CJC, Fauchereau N (2008) Extreme rainfall in the Namib Desert during summer 2006 and influences of regional ocean variability. Int J Climatol 28:1061–1070. doi:10.1002/joc.1603

Philippon N, Rouault M, Richard Y, Favre A (2012) The influence of ENSO on winter rainfall in South Africa. Int J Climatol 32:2333–2347. doi:10.1002/joc.3403

Pohl B, Fauchereau N, Reason CJC, Rouault M (2010) Relationships between the Antarctic Oscillation, the Madden-Julian Oscillation, and ENSO, and consequences for rainfall analysis. J Clim 23:238–254

Pohl B, Rouault M, Sen Roy S (2014) Similation of the annual and diurnal cycles of rainfall over South Africa by a regional climate model. Clim Dyn 43:2207–2226. doi:10.1007/s00382-013-2046-8

Reason CJC, Rouault M (2005) Links between the Antarctic Oscillation and winter rainfall over western South Africa. Geophys Res Lett 32:L07705. doi:10.1029/2005GL022419

Reason CJC, Allan RJ, Lindesay JA, Ansell TJ (2000) ENSO and climatic signals across the Indian Ocean basin in the global context: part I, interannual composite patterns. Int J Climatol 20:1285–1327

Reason CJC, Rouault M, Melice JL, Jagadheesha D (2002) Interannual winter rainfall variability in SW South Africa and large scale ocean–atmosphere interactions. Meteorol Atmos Phys 80:19–29

Rouault M, White SA, Reason CJC, Lutjeharms JRE, Jobard I (2002) Ocean–atmosphere interaction in the Agulhas current region and a South African extreme weather event. Weather Forecast 17:655–669

Schuenemann KC, Cassano JJ, Finnis J (2009) Synoptic forcing of precipitation over Greenland: climatology for 1961–99. J Hydrometeorol 10:60–78

Singleton AT, Reason CJ (2006) Numerical simulations of a severe rainfall event over the Eastern Cape coast of South Africa: sensitivity to sea surface temperature and topography. Tellus 58:355–367

Singleton AT, Reason CJ (2007a) A numerical model study of an intense cutoff low pressure system over South Africa. Mon Weather Rev 135:1128–1150

Singleton AT, Reason CJ (2007b) Variability in the characteristics of cut-off low pressure systems over subtropical southern Africa. Int J Climatol 27:295–310

Smith TM, Reynolds RW, Peterson TC, Lawrimore J (2008) Improvements to NOAA's historical merged land-ocean surface temperature analysis (1880–2006). J Clim 21:2283–2296

Taljaard JJ (1985) Cut-off lows in the South African region. South African Weather Bureau, Technical paper 14

Taljaard JJ (1995) Atmospheric circulation systems, synoptic climatology and weather phenomena of South Africa. Part 2: atmospheric circulation systems in the South African region. South African Weather Bureau, Technical paper 28

Taljaard JJ (1996) Atmospheric circulation systems, synptic climatology and weather phenomena of South Africa. Part 6: Rainfall in South Africa. South African Weather Bureau, Technical paper 32

Tennant WJ, Reason CJC (2005) Associations between the global energy cycle and regional rainfall in South Africa and Southwest Australia. J Clim 18:3032–3047

Todd M, Washington R, Palmer PI (2004) Water vapour transport associated with tropical-temperate trough systems over southern Africa and the southwest Indian Ocean. Int J Climatol 24:555–568

Tozuka T, Abiodun BJ, Engelbrecht FA (2014) Impacts of convection schemes on simulating tropical-temperate troughs over southern Africa. Clim Dyn 42:433–451

Van Heerden J, Terblance DE, Schulze GC (1988) The Southern Oscillation and South African summer rainfall. J Clim 8:577–597

Washington R, Preston A (2006) Extreme wet years over southern Africa: role of Indian Ocean sea surface temperatures. J Geophys Res 111:D15104. doi:10.1029/2005JD006724

Washington R, Todd M (1999) Tropical-temperate links in the Southern African and southwest Indian Ocean satellite-derived daily rainfall. Int J Climatol 19:1601–1616

Weldon D, Reason CJC (2014) Variability of rainfall characteristics over the South Coast region of South Africa. Theor Appl Climatol 115:177–185. doi:10.1007/s00704-013-0882-4

Wilks DS (2011) Statistical methods in the atmospheric sciences, 3rd edn. Academic Press, Amsterdam